Excimer Laser Gain By Pulse Shape Analysis

GERD MAROWSKY, MARTIN MUNZ, AND FRANK K. TITTEL, SENIOR MEMBER, IEEE

Abstract—**An analysis of the temporal emission of broadband tunable excimer lasers such as Xe_2Cl shows that the laser pulse can be described in terms of a Q-switch model rather than by steady-state considerations. For electron-beam (e-beam) pumped rare gas halide mixtures, transient absorption of the majority gas—usually argon—acts as a *chemical Q-switch*. The ring-up time of the delayed laser pulse may be conveniently used for optimization of the laser gas mixture.**

Introduction

FOR the prediction of laser performance and optimization of the cavity configuration, a knowledge of the optical gain of a particular active medium is essential [1]. Small-signal gain is characterized by the product $N^*\sigma_e$ where N^* is the excited state population density and σ_e is the cross section for stimulated emission. With prior knowledge of σ_e from fluorescence data of the transition of interest such as the bandwidth and spontaneous decay time [2], a measurement of $g \equiv N^*\sigma_e$ allows a determination of the population density of the upper laser level and thus eventually facilitates kinetic modeling of the excitation process responsible for build-up of inversion.

Gain measurements are relatively straightforward for high-gain systems by application of amplified spontaneous emission (ASE) techniques [3], [4]. Medium- and low-gain systems require more refined procedures such as multiple passage probing of gain or loss by means of a laser beam. Yet another approach is to analyze the temporal behavior of the laser output making use of the largest number of possible roundtrips. Medium- and low-gain candidates are the recently discovered broadband emitting tunable excimer lasers, in particular, the $C \rightarrow A$ transition of XeF [5]-[7] and the triatomic excimers such as Xe_2Cl [8], [9] and Kr_2F [10]. Several interesting characteristics of the temporal behavior of trimer emission are apparent from Fig. 1(a) (see also [11]): (1) the rapid build-up of the diatomic excimer emission of the $B \rightarrow X$ transition of XeCl centered at 308 nm upon electron-beam (e-beam) excitation (the e-beam pulse is shown as the Faraday-cup probe current), (2) the almost simultaneous occurrence of triatomic Xe_2Cl fluorescence, and (3) the considerably delayed Xe_2Cl laser pulse with typical delay times of $\approx$40 ns.

Manuscript received February 27, 1981. This work was supported in part by the Office of Naval Research, the Robert A. Welch Foundation, and the National Science Foundation.

G. Marowsky is with the Max Planck Institute für Biopysikalische Chemie, Abteilung Laserphysik, Postfach 968, D-3400 Göttingen, Germany.

M. Munz is with the Institut für Theoretische Physik der Universitat Stuttgart, Stuttgart, Germany.

F. K. Tittel is with the Department of Electrical Engineering, Rice University, Houston, TX 77001.

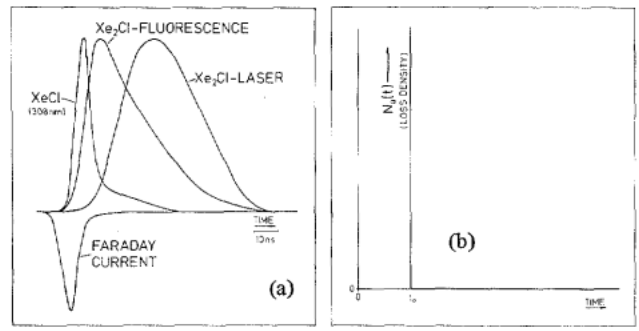

Fig. 1. (a) Typical temporal characteristics of XeCl- and Xe_2Cl-fluorescence and laser pulses. The e-beam excitation pulse, as monitored by a Faraday current probe, is also indicated. (b) Assumption of a fast Q-switch model: the loss density $N_a(t)$ vanishes at $t = t_0$.

The purpose of this paper is an explanation of the described temporal behavior of fluorescence and laser emission and a gain determination by analysis of the laser pulse shape, in particular, by analysis of the *pulse ring-up time*. Other parameters of interest are predictions concerning the delay time and maximum available power density from such a system.

Theoretical Model

The theoretical model is based on the assumption that the effective gain g_{eff} can be expressed by the equation

$$g_{\text{eff}} \equiv N^*(t)\,\sigma_e - N_a(t)\,\sigma_a \tag{1}$$

with N_a as the density of absorbers of cross sections σ_a. At time $t = t_0$ [see Fig. 1(b)], which coincides approximately with the peak of the observed fluorescence, $N_a(t)$ vanishes because of natural decay or chemical decomposition of the absorbing species. In the case of e-beam pumped rare gas halide mixtures this initial absorption can be attributed to a fast decaying absorbing species of the majority gas argon [12]. After $t = t_0$ the build-up of the laser pulse $I_1(t)$, which corresponds to the photon flux inside the cavity, can be described by a set of rate equations known from Q-switch theory [13], [14]:

$$\dot{N}^* = -\sigma_e N^* I_1(t) \tag{2}$$

$$\dot{I}_1(t) = cI_1(t)(\sigma_e N^* - \kappa). \tag{3}$$

In (3) c denotes the velocity of light and $\kappa = \kappa_a + \kappa_i$ are the losses due to outcoupling (κ_a) and other non-resonant, internal losses (κ_i). For a cavity of length L (cf. Fig. 2) and mirrors of reflectivity R_1 and R_2, the quantity κ_a is given by [1]

$$\kappa_a = \frac{1}{2L} \ln\left(\frac{1}{R_1} \cdot \frac{1}{R_2}\right). \tag{4}$$

0018-9197/81/0700-1281$00.75

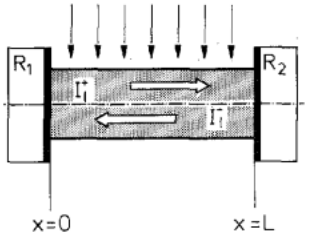

Fig. 2. Configuration of transversely excited active volume of length L, surrounded by mirrors of reflectivity R_1 and R_2.

For $R_1 = 1$ and $R_2 = R$, the externally observed output power density P_1 is given by [1]

$$P_1 = h\nu_1 \cdot \frac{1-R}{1+R} \cdot I_1 \tag{5}$$

where $h\nu_1$ is the energy per photon.

Equations (2) and (3) incorporate the usual assumptions for fast Q-switching: neglecting the effect of population relaxation and pumping during the laser pulse, as shown in Fig. 3. In order to check the validity range of the equations for the Q-switch model, we first present a derivation that starts from the more general photon transport equation for $I_1(x, t)$:

$$\frac{1}{c} \cdot \frac{\partial}{\partial t} \cdot I_1^{\pm}(x, t) \pm \frac{\partial}{\partial x} \cdot I_1^{\pm}(x, t) = I_1^{\pm} g(I_1^{\pm}). \tag{6}$$

Here I_1^+ and I^- are the internal intensities propagating in the positive and negative x-direction, as shown in Fig. 2, where the total (internal) intensity I_1 at any point is given by

$$I_1 = I_1^+ + I_1^-. \tag{7}$$

According to [1] $g(I_1)$ is determined by the relation

$$g(I_1) \equiv \sigma_e N^*(I_1) - \kappa_i. \tag{8}$$

Equation (6) can be separated by letting

$$I_1^{\pm}(x, t) = X^{\pm}(x) \cdot T^{\pm}(t) \tag{9}$$

which yields the following equation for $X^{\pm}(x)$ and $T^{\pm}(t)$:

$$\frac{1}{c} \cdot \frac{1}{T^{\pm}} \cdot \frac{\partial T^{\pm}}{\partial t} - g(I_1) = \mp \frac{1}{X^{\pm}} \cdot \frac{\partial X^{\pm}}{\partial x}. \tag{10}$$

For $I_1 \neq I_1(x)$, both sides of (10) are constant:

$$\pm \frac{1}{X^{\pm}} \cdot \frac{\partial X^{\pm}}{\partial x} = \bar{c} \tag{11}$$

or

$$X^{\pm}(x) = X^{\pm}(0) \cdot e^{\pm \bar{c} x}. \tag{12}$$

Insertion of (12) into (6) leads to

$$\frac{1}{c} \cdot \frac{\partial T^{\pm}}{\partial t} = T^{\pm}[g(I_1) - \bar{c}], \tag{13}$$

or with

$$I_1(t) = T^+ + T^-, \tag{14}$$

$$\frac{1}{c} \cdot \frac{\partial I_1}{\partial t} = I_1[g(I_1) - \bar{c}]. \tag{15}$$

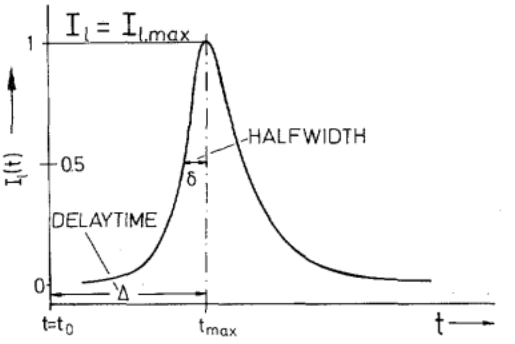

Fig. 3. Typical excimer laser pulse, characterized by a maximum internal photon flux $I_{1,\max}$, a delay time Δ, and a half-width δ.

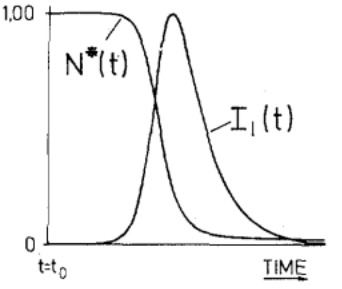

Fig. 4. Computer solution of (2) and (3) showing the typical temporal shape of $I_1(t)$ and $N^*(t)$ with $N^*(t_0)$ normalized to $I_{1,\max}$.

A comparison with the stationary solutions of [1] leads to $\bar{c} \equiv \kappa_a$ and (15) can be rewritten in terms of the formulation according to (3):

$$\frac{1}{c} \cdot \frac{dI_1}{dt} = I_1[N^*(I_1) \cdot \sigma_e - (\kappa_a + \kappa_i)]. \tag{16}$$

The derivation of (16) from the more general photon transport (6) is based on the assumption $I_1 \neq I_1(x)$, which is justified only for medium- and low-gain media. Consequently, application of (2) and (3) is limited to laser resonators with high cavity-Q or a reflectivity R close to unity.

After dividing (2) by (3),

$$\frac{dN^*}{dI_1} = -\frac{1}{c} \cdot \frac{\sigma_e N^*(t)}{(\sigma_e N^*(t) - \kappa)}, \tag{17}$$

$I_1(t)$ and $N^*(t)$ can be written as follows:

$$I_1(t) = I_1(0) - \frac{c}{\sigma_e}\left[\sigma_e N^*(t) - \sigma_e N^*(0) + \kappa \cdot \ln\frac{N^*(0)}{N^*(t)}\right] \tag{18}$$

$$\int_{N^*(0)}^{N^*(t)} \frac{dN^*}{\sigma_e N^*\left[c(N^* - N^*(0)) - I_1(0) + \frac{c\kappa}{\sigma_e} \cdot \ln\frac{N^*(0)}{N^*(t)}\right]} = \int_0^t dt' = t. \tag{19}$$

Formally, (19) together with (18) represents the exact solution of the Q-switch problem, with the time dependence $N^*(t)$ and $I_1(t)$, as depicted in Fig. 4, in agreement with [13]-[15]. Both an approximate solution (19) and a numer-

ical computer solution with the experimental data described in the following section indicate that a very good approximation may be obtained with the following assumptions:

(a) leading edge of the laser pulse:

$$N^*(t) \approx N^*(0)$$

or

$$I_1(t) = I_1(0) \cdot \exp\{ct[N^*(0)\,\sigma_e - \kappa]\}; \tag{20}$$

(b) trailing edge of the laser pulse:

$$N^*(t) \approx 0$$

or

$$I_1(t) = I_{1,\max} \cdot \exp(-c\kappa t). \tag{21}$$

In other words, for a low-gain laser system the ring-up time is essentially given by the difference between gain and cavity losses and the pulse decay time by the product $c(\kappa_a + \kappa_i)$, usually called the cavity decay time.

It is interesting to note that the maximum of the internal laser intensity $I_{1,\max}$ as derived from (18), is obtained for

$$N^*(t) \equiv \kappa/\sigma_e \tag{22}$$

or $N^*(t) = N^*_{\text{station}}$, which is the value for N^* under *steady-state conditions* of laser operation:

$$I_{1,\max} = I_1(0) + \frac{c}{\sigma_e}\{g - \kappa(1 + \ln(g/\kappa))\} \tag{23}$$

where $g \equiv N^*(0)\,\sigma_e$.

Results

For the example of gain analysis of the triatomic excimer Xe_2Cl, let us consider a transversely excited active volume $V_a = 10$ cm^3 and length $l = 10$ cm with $R_1 = 1$ and $R_2 = 0.95$, based on the experimental conditions described in [9]. The small-signal gain $g \equiv N^*(0) \cdot \sigma_e$ is given by $N^*(0) = 8 \cdot 10^{14}$ cm^{-3} and $\sigma_e = 10^{-17}$ cm^2, or $g = 8 \cdot 10^{-2}$ per pass. For a spontaneous decay time $\tau = 135$ ns [8], [11], the total spontaneous decay rate $N^* \cdot V_a/\tau$ is approximately $5 \cdot 10^{22}$ s^{-1}. A photon flux of $5 \cdot 10^{22}$ cm$^{-2} \cdot$ s^{-1} is the upper limit of the quantity $I_1(0)$ in (23) and a value of 10^{20} cm$^{-2} \cdot$ s^{-1} is a more practical figure. In Fig. 5 we have studied the influence of various assumptions concerning $I_1(0)$ on three quantities of interest: $I_{1,\max}$, delay time Δ, and halfwidth δ of the laser pulse. It is apparent from this figure that $I_1(0)$ does not influence the peak intensity $I_{1,\max}$ and the halfwidth δ. However, $I_1(0)$ influences the delay time Δ which is an experimental quantity that is difficult to determine. Fig. 6 depicts the dependence of $I_{1,\max}$, δ, and Δ on the inversion density $N^*(0)$ for an initial photon flux $I_1(0)$, due to spontaneous decay of 10^{21} cm$^{-2} \cdot$ s^{-1}. The internal maximum power density $I_{1,\max}$ and the halfwidth δ for the case $N^*(0) = 8 \cdot 10^{14}$ cm^{-3} are also shown, which results in $I_{1,\max} = 0.2$ MW/cm^2 for an Xe_2Cl emission wavelength of 500 nm and $\delta = 13.6$ ns. Fig. 7 shows a compilation of laser pulses obtained by a computer solution of (2) and (3) for different values of $N^*(0)$ close to $N^*(0) = 8 \cdot 10^{14}$. The internal photon flux $\hat{I}_1$ has been normalized to the value obtained for $N^*(0) = 12.5 \times 10^{14}$ cm^{-3}. The figure clearly shows the influence of $N^*(0)$, or the initial gain, on the shape of the laser pulse and the delayed occurrence of the pulse as characterized by Δ.

We next consider the difference in actual output power

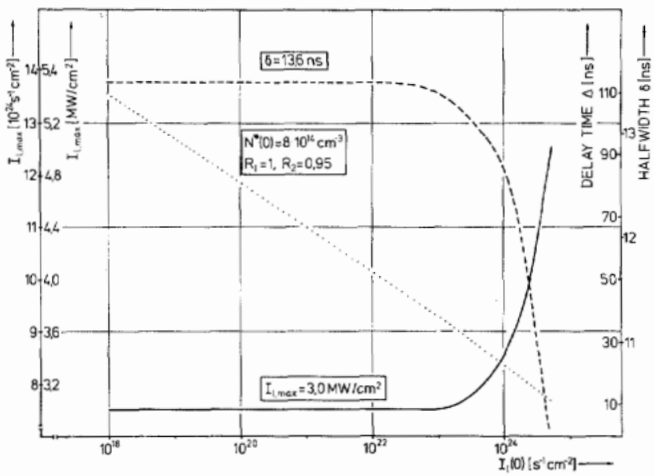

Fig. 5. Influence of $I_1(0)$ on $I_{1,\max}$, Δ, and δ for $N^*(0) = 8 \cdot 10^{14}$ cm^{-3}.

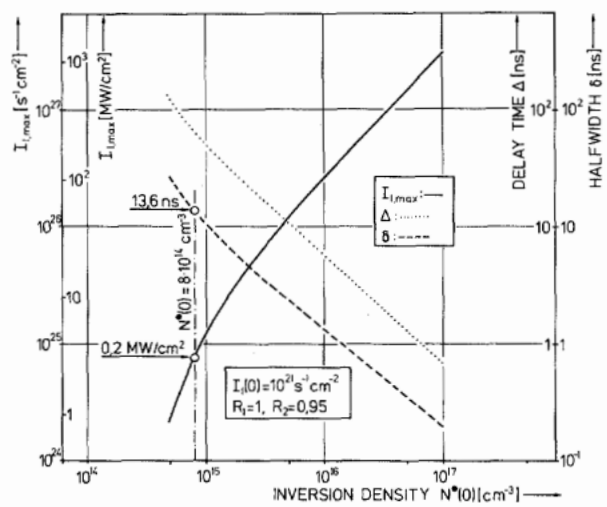

Fig. 6. Dependence of $I_{1,\max}$, Δ, and δ on the initial inversion density $N^*(0)$ with $I_1(0) = 10^{21}$ cm$^{-2} \cdot$ s^{-1}. The power density (MW/cm^2) has been calculated for a wavelength $\lambda = 500$ nm.

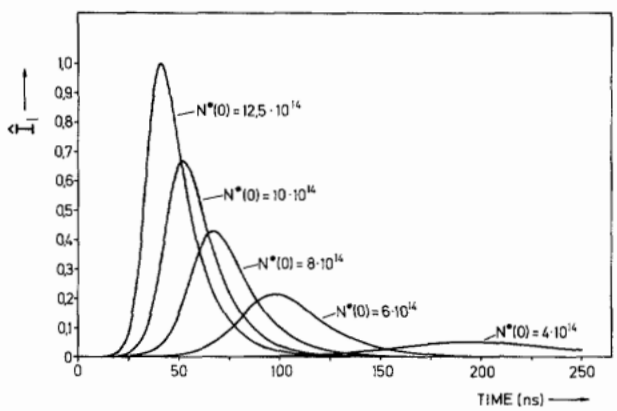

Fig. 7. Temporal characteristics of laser pulses for five different initial inversion densities $N^*(0)$ close to $8 \cdot 10^{14}$ cm^{-3} and normalized to $I_{1,\max} \equiv \hat{I}_1$; ($N^*(0) = 12.5 \times 10^{14}$).

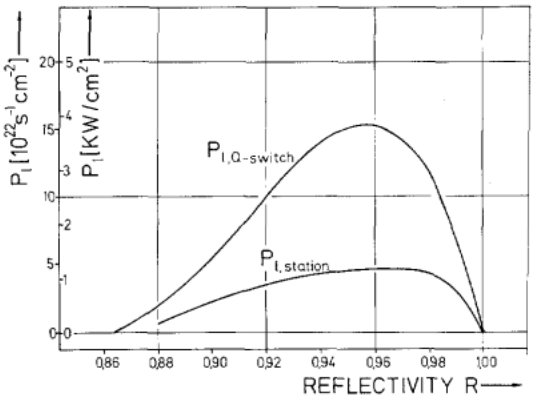

Fig. 8. Comparison of output power densities for steady-state laser conditions ($P_{1,\text{station}}$) and the Q-switched model ($P_{1,Q\text{-switch}}$).

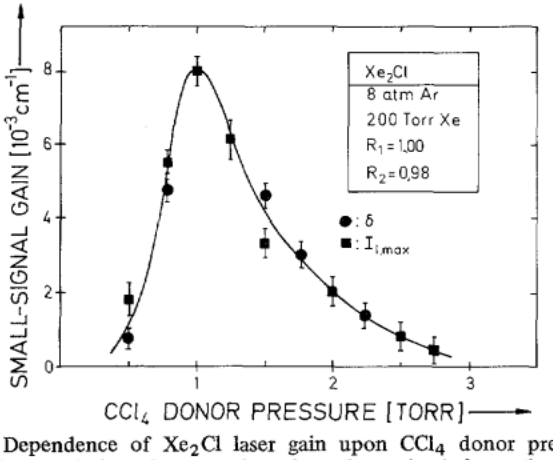

Fig. 9. Dependence of Xe_2Cl laser gain upon CCl_4 donor pressure. Circular symbols refer to gain values determined from the pulse ring-up time as characterized by the halfwidth δ; rectangular symbols refer to an evaluation of $I_{1,\max}$. The solid curve represents a fit to experimental data.

density P_1 for *steady-state operation* of the described laser system and for Q-switched conditions. In the latter case $P_1 \equiv P_{1,Q\text{-switch}}$ is given by

$$P_{1,Q\text{-switch}} = h\nu_1 \cdot \frac{1-R}{1+R} \cdot I_{1,\max}(g,R) \tag{24}$$

where $I_{1,\max}(g,R)$ is given by (23). Stationary conditions $P \equiv P_{1,\text{station}}$ are given by [1]

$$P_{1,\text{station}} = h\nu_1 \cdot \frac{1-R}{1+R} \cdot \frac{1}{\sigma_e \tau} \cdot \left\{ \frac{g_{\text{station}}}{\kappa} - 1 \right\} \tag{25}$$

with τ, as before, the spontaneous decay time, κ as defined by (4), and g_{station} as the steady-state gain produced by the excitation source. A comparison of (24) and (25) in Fig. 8 shows that the output power density for Q-switch laser operation up to 4 kW/cm^2 for $R = 0.95$ exceeds $P_{1,\text{station}}$ by only a factor of four.

Experimental data depicting optimization of the Xe_2Cl laser output by varying the CCl_4 donor pressure at a fixed partial pressure of 8 atm of the main buffer gas Ar and 200 torr of Xe is shown in Fig. 9 (further details are given in [11]). This figure shows the good agreement between experimental data points obtained by deriving the gain from the ring-up time δ or by determining the CCl_4 pressure dependence of the output power density according to (24). For an output coupler of $R = 0.98$, a power density $P_1^{\max}$ of 3 kW/cm^2 is obtained which is in agreement with the results shown in Fig. 8. The gain peaks at a CCl_4 donor pressure of 1 torr at a value of $8 \cdot 10^{-3}$ cm^{-1}.

Conclusion

Based on the approximate closed form and numerical computer solution of the rate equations, it has been shown that the temporal behavior of a low-gain laser system such as the triatomic Xe_2Cl can be described in terms of a Q-switch model. The initial losses that prevent the system from laser oscillation are due to transient absorption of the e-beam excited rare gas mixture. The output power density and delayed onset of the laser pulse have been considered. Details of a gain determination based on pulse shape analysis are given which is valid provided that there is no spatial variation of the photon flux inside the cavity. In addition, the gain data does not depend on any assumptions concerning the unknown photon flux along the cavity axis.

Acknowledgment

The authors wish to thank G. Haag for helpful discussions. Previous work performed by W. K. Bischel and D. J. Eckstrom on gain analysis of the XeF $C \rightarrow A$ laser initiated these studies for the triatomic excimers [16]. Helpful assistance in performing the Xe_2Cl experiments at Rice University by W. L. Wilson and M. Smayling is also acknowledged.

References

[1] M. Munz, G. Haag, and G. Marowsky, "Optimization of dye-laser output coupling by consideration of the spatial gain distribution," *Appl. Phys.*, vol. 22, pp. 175–184, 1980.
[2] C. A. Brau, "Rare gas halogen lasers," in *Excimer Lasers*, C. K. Rhodes, Ed. Berlin: Springer-Verlag, 1979.
[3] C. V. Shank, "Physics of dye lasers," *Rev. Mod. Phys.*, vol. 47, pp. 649–658, 1975.
[4] G. Marowsky, F. K. Tittel, W. L. Wilson, and E. Frenkel, "Laser gain measurements by means of amplified spontaneous emission," *Appl. Opt.*, vol. 19, pp. 138–143, 1980.
[5] W. E. Ernst and F. K. Tittel, "Gain studies of electron beam excited XeF laser mixtures," *IEEE J. Quantum Electron.*, vol. QE-16, pp. 945–948, Sept. 1980.
[6] R. M. Hill, P. L. Trevor, D. L. Huestis, and D. C. Lorents, "Measurement of gain on the XeF ($C-A$) blue green band," *Appl. Phys. Lett.*, vol. 34, pp. 137–139, 1979.
[7] W. K. Bischel, H. H. Nakano, D. J. Eckstrom, R. M. Hill, D. L. Huestis, and D. C. Lorents, "A new blue-green excimer laser in XeF," *Appl. Phys. Lett.*, vol. 34, pp. 565–567, 1979.
[8] K. Y. Tang, D. C. Lorents, and D. L. Huestis, "Gain measurements on the triatomic excimer Xe_2Cl," *Appl. Phys. Lett.*, vol. 36, pp. 347–349, 1980.
[9] F. K. Tittel, W. L. Wilson, R. E. Stickel, G. Marowsky, and W. Ernst, "A triatomic Xe_2Cl excimer laser in the visible," *Appl. Phys. Lett.*, vol. 36, pp. 405–407, 1980.
[10] F. K. Tittel, M. Smayling, W. L. Wilson, and G. Marowsky, "Blue laser action by the rare gas halide trimer Kr_2F," *Appl. Phys. Lett.*, vol. 37, pp. 862–864, 1980.
[11] —, *IEEE J. Quantum Electron.*, to be published.
[12] E. Zamir, D. L. Huestis, H. H. Nakano, R. M. Hill, and D. C. Lorents, "Visible absorption by electron-beam pumped rare gases," *IEEE J. Quantum Electron.*, vol. QE-15, pp. 281–288, May 1979.
[13] W. G. Wagner and B. A. Lengyel, "Evolution of the giant pulse in a laser," *J. Appl. Phys.*, vol. 34, pp. 2042–2046, 1963.
[14] R. W. Hellwarth, "Control of fluorescent pulsations," in *Advances in Quantum Electronics*, J. R. Singer, Ed. New York: Columbia, 1961, p. 334.

[15] B. A. Lengyel, *Lasers*, 2nd ed. New York: Wiley, 1971, pp. 182–190.
[16] W. K. Bischel, D. J. Eckstrom, D. L. Huestis, and D. C. Lorents, presented at Lasers '79, Orlando, FL, Dec. 12–21, 1979.

Gerd Marowsky, for a photograph and biography, see page 356 of the March 1981 issue of this JOURNAL.

Martin Munz, for a photograph and biography, see page 356 of the March 1981 issue of this JOURNAL.

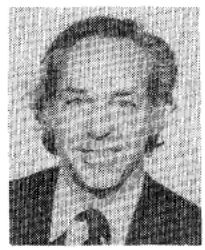

Frank K. Tittel (SM'72) was born in Berlin, Germany, in 1933. He received the M.A. and Ph.D. degrees in physics from Oxford University, Oxford, England.

From 1959 to 1967 he was a Research Physicist at the General Electric Research and Development Center, Schenectady, NY. Since 1967 he has been at Rice University, Houston, TX, where he is a Professor of Electrical Engineering. His research interests include laser devices, nonlinear optics, and laser spectroscopy.

Dr. Tittel is a member of the Optical Society of America and the American Physical Society.

Surface Raman Ellipsometry

GARY L. EESLEY, MEMBER, IEEE

Abstract—**A method for achieving the ultrahigh sensitivity required for surface vibrational spectroscopy is proposed. Polarization selective heterodyne detection permits shot-noise limited submonolayer detection with classically noisy picosecond laser sources. Furthermore, the polarization selectivity is used to eliminate the overwhelming thermally induced changes in surface reflectivity.**

I. INTRODUCTION

THE application of Raman spectroscopy to studies of atomic and molecular interactions at surfaces is becoming more important, since practical situations (catalytic gas flows, electrochemical cells, etc.) are inaccessible to electron spectroscopies which require ultrahigh vacuum environments [1]. This importance is emphasized by the fact that Raman spectra can be used to identify adsorbed species as well as to determine the bond strengths and bonding geometry (from force constant calculations). The high-frequency resolution of Raman spectroscopy ($\sim$1 cm^{-1} = 0.12 meV) will allow the differentiation between subtle changes in the state of surface species as well.

Observations of an anomalous 10^4-10^6 enhancement in Raman scattering from molecules adsorbed on silver surfaces was originally thought to improve the feasibility of Raman scattering as a surface vibrational probe. However, this enhancement appears to be confined to molecules adsorbed on roughened Ag, Cu, and Au surfaces [2], and is thus not generally applicable. In an effort to overcome the poor sensitivity of spontaneous Raman scattering, Levine *et al.* [3] have recently proposed and analyzed methods for acquiring surface vibrational spectra by means of stimulated Raman spectroscopy (SRS). Furthermore, Levine and Bethea [4] have constructed an SRS system comprised of a pair of synchronously mode-locked picosecond dye lasers. After extensive developmental work, they claim to have achieved the sensitivity necessary for the detection of submonolayer quantities of molecules adsorbed on various metal and dielectric substrates.

A key obstacle to achieving this sensitivity is the requirement that the probe laser classical power fluctuations be reduced below the quantum statistical power fluctuations (shot noise) [5]-[7]. In addition to this requirement, it is also realized that the signal amplitude (or Raman gain) must exceed the shot noise, and this requires the use of pump laser intensities on the order of 100 MW/cm^2. Unfortunately, such high intensities can produce substrate temperature changes which result in relatively large changes in surface reflectivity in the case of metals [8]. As an example, Levine *et al.* [3] found that the required pump laser intensities would produce a Raman gain of $\sim 10^{-8}$, whereas the change in surface reflectivity was $\sim 10^{-4}$. Since the gain signal is observed in reflection, the pump laser induced change in reflectivity will obscure the weak Raman gain signal and, in order to minimize this effect, picosecond laser pulses are required.

Levine *et al.* [4] achieve the shot-noise limit as well as eliminate most of the thermal background signal by utilizing a novel and complex laser amplitude and frequency modulation scheme. Although the ultrahigh sensitivity of this system is impressive, the sophisticated optical and electronic measures required may not be justified by the signal-to-noise (S/N) improvement.

Manuscript received January 27, 1981.
The author is with the Department of Physics, General Motors Research Laboratories, Warren, MI 48090.

0018-9197/81/0700-1285$00.75